Combining genome-scale *Drosophila* 3D neuroanatomical data by bridging template brains

James D. Manton[1,3], Aaron D. Ostrovsky[1,3,4], Lea Goetz[1,3,5], Marta Costa[1,3], Torsten Rohlfing[2], Gregory S. X. E. Jefferis[1,*]

[1]Division of Neurobiology, MRC Laboratory of Molecular Biology, Cambridge, CB2 0QH, UK.

[2]SRI International, Neuroscience Program, Center for Health Sciences, Menlo Park, CA, USA.

[3]These authors contributed equally.

[4]Present address: Centre for Organismal Studies, Im Neuenheimer Feld 329, Heidelberg University, 69120 Heidelberg, Germany.

[5]Present address: Wolfson Institute for Biomedical Research, University College London, Gower Street, London, WC1E 6BT, UK.

Please note that this preprint is a public draft not a submitted manuscript. It is released in the expectation that it will be useful to our colleagues as is and in order to solicit feedback. All presented results are considered reliable, but it is likely that the final manuscript may contain some additional analysis; for this reason, the byline should not be considered final. There are some omissions in the Introduction and especially Discussion sections of the manuscript, particularly with respect to citations to the literature. Please note that current versions of the open source software described in the manuscript are available by following links in the Methods. Likewise nearly all data are also immediately available; some residual data will be made available online no later than the eventual publication of the manuscript. We welcome feedback, queries and suggestions on any aspect of the manuscript to jefferis@mrc-lmb.cam.ac.uk.

Abstract

The stereotyped structure of mammalian and invertebrate brains is a crucial determinant of their circuit organization. Thus large scale efforts to map circuit organization using 3D image data are underway in a number of model systems, including flies and mice. Many of these studies use registration of sample images to a standard template brain to enable co-visualization and spatial querying. However, studies often use distinct template brains, resulting in large islands of data which cannot be directly compared. To enable this comparison, we have constructed bridging registrations between template brains accounting for the vast majority of *Drosophila melanogaster* 3D neuroanatomical data. Furthermore, we solve the related problem of mapping data between the left and right brain hemispheres via the construction of mirroring registrations. Finally, we extend our approach across species to demonstrate its potential use in evolutionary studies of neural circuit structure and provide bridging registrations that link a new set of template brains generated for four *Drosophila* species that are divergent over 40 million years of evolution.

We describe our strategy, document the freely available anatomical data and open source computer tools that we have generated and provide numerous examples of their use. This effort has unified data from over 30,000 publicly available images, with resources including the 3D atlas embodying the new standard *Drosophila* anatomical nomenclature and the largest single neuron databank yet available in any species. Over 20,000 registered images have been contributed to the Virtual Fly Brain project and can be viewed online at www.virtualflybrain.org.

Contents

List of Tables

List of Figures

1 Introduction

To describe the structure and organization of neuronal circuits, neuroscience increasingly makes use of 3D brain atlases. These provide a standardized space, often described as a template brain or standard brain, that enables direct comparison between different structures — from the morphology of individual neurons, to microcircuits and potentially whole connectomes — in the space of the brain as a whole. Furthermore, these approaches enables comparisons between different brains, such as the circuit geometry in a diseased state compared to that of a normal brain, or longitudinal studies of the same individuals.

Template brains and associated data have been generated for a wide variety of species. For example templates are available for insect brains, including the honeybee *Apis mellifera* (Brandt et al., 2005), the moths *Schistocerca gregaria* (Kurylas et al., 2008) and *Manduca sexta* (El Jundi et al., 2009), the locust *Heliothis virescens* (Kvello et al., 2009), and the flour beetle *Tribolium castaneum* (Dreyer et al., 2010). Brain atlases are also available for many higher animals, including the zebrafish *Danio rerio* (Wullimann et al., 1996), the mouse C57BL/6 (Lein et al., 2007) , the red junglefowl chick *Gallus domesticus* (Kuenzel and Masson, 1988), and humans (Holmes et al., 1998; Rohlfing et al., 2010; Talairach and Tournoux, 1988). Now large-scale projects are underway aiming for the "anatomical reconstruction of neural circuits at all scales" (BRAIN Working Group, 2014). Therefore, robust and well-tested methods for generating and analyzing the anatomical data from brain atlases are required.

One vital approach in the construction and subsequent application of most modern brain atlases, is image registration, where images are transformed to match the structure of a canonical template brain. The importance of image registration is now well appreciated (Peng et al., 2011; Tomer et al., 2010), with much effort being expended on improving registration methods in terms of speed and accuracy (Avants et al., 2008; Klein et al., 2010; Rohlfing and Maurer, 2003; Rueckert et al., 1999). Although most individual studies use just one template brain to which all data is registered, there are typically multiple such templates in use within a given area of neuroscience; this can be due to experimental differences in data acquisition as well as historical or other non-scientific reasons.

Despite this, the practicalities of transforming data between different template brains has received comparatively little attention. Although it is possible to re-register data from one study against a different template brain, this can be difficult and very time consuming and generally results in some specimens failing to register adequately; furthermore the imaging modality may be different and not directly comparable. These are strong arguments of the construction of single *bridging* registrations to map data from one template brain to another without requiring the time-consuming re-registration of the original data.

One of the first examples of bridging in neuroanatomy is the that of Brett et al. (2001), in which SPM99 was used to create an affine transformation between the Talairach and MNI templates of the human brain. This resulted in a registration that, while giving good alignment of the brain surfaces, had relatively poor alignment of internal structures due to the different shapes of the brain. Carmack et al. (2004) improved the alignment for deep brain areas via an alternative affine transformation at the cost of poorer surface alignment. As noted by the original authors, "no affine transformation exists that will satisfactorily improve Talairach and MNI brain agreement on a global level", suggesting that an alternative approach must be taken for best results. Lacadie et al. (2008) improved on previous attempts at bridging the Talairach and MNI atlases via the use of a non-linear registration, but only used the surfaces of the brains for alignment, leaving many deep brain misalignments relatively uncorrected. Other attempts have used piece-wise linear mappings, in which different brain substructures are subjected to independent affine transforms (e.g. the first *Drosophila* standard template brain, Rein et al., 2002), but as the transformations are independent it is possible for two locations in the original brain to map to the same location in the reference brain.

Fully non-rigid 'warping' deformations can avoid this issue at the expense of increased computational cost. Here, a number of different methods are used to construct a deformation that better matches substructures of the two brains, with approaches including diffeomorphisms (Avants et al., 2008), physical continuum models (Christensen et al., 1996), optical flow (Lefébure and Cohen, 2001) and B-splines (Rohlfing et al., 2003; Rueckert et al., 1999). With continuously increasing computational power, the time taken to compute warping registrations is rapidly decreasing and so non-rigid

warping registrations are becoming the de-facto standard for image registration across all disciplines (Peng et al., 2011).

Of all model organisms used in neuroscience, *Drosophila melanogaster* has by far the greatest wealth of 3D datasets publicly available, including GAL4 expression patterns (Jenett et al., 2012), single neuron images (Chiang et al., 2011), neuronal tracings (Grosjean et al., 2011; Jefferis et al., 2007; Kohl et al., 2013), neuroblast clone images (Cachero et al., 2010; Ito et al., 2013; Yu et al., 2013), and neuropil segmentations (Ito et al., 2014). For each of these studies, data were registered against a template brain, typically one generated within the lab of the authors (detailed in Table 1). While this enables the comparison of data within a dataset, the fact that each template brain is different means that data across studies cannot be directly compared, except 'by eye'.

We have created fully non-rigid bridging registrations that make it possible to transform data from one reference brain to another, bringing them into a common 3D coordinate space, along with mirroring registrations that take data from one side of a reference brain to the other. We provide numerous examples of the use of these bridging registrations, along with open source software that enables them to be applied simply and at scale to a variety of data. We have applied these approaches to all the large *Drosophila* datasets that are publicly available. In two of the largest cases, only raw unregistered data were available, so we began by registration to an appropriate template brain. This has allowed us to deposit over 20,000 co-registered images from different sources in the virtualflybrain.org project. Where the original authors permit this, we have made these registered data available for direct download; where this was not possible scripts for transformation and appropriate registrations are provided.

While we have developed our methods for *Drosophila* neuroanatomy, our approach generalizes to other species, providing powerful tools for combining future datasets within species. In addition, we show that it is possible to bridge data across species within the *Drosophila* genus. This enables us to describe the conservation of gross anatomical features in higher brain regions, including substantial sexual dimorphisms, and to co-locate other data such as single neurons and surface models with those data.

2 Results

2.1 Overview of Drosophila template brains and registered data

Two approaches have been taken in specifying template brains for the various datasets available: either a specific brain image has been chosen as a canonical brain, or a number of brain images have been selected and averaged to produce a synthetic canonical brain. Choosing a single brain avoids any potential artifacts generated by the averaging procedure, but an average brain reduces staining inhomogeneities and deformations introduced during the staining, fixing and general handling of the brain, thus increasing the likelihood of successful and accurate registration. Quantitative neuroanatomical work requires images to be spatially calibrated, but such calibrations are not present in all template brains.

Table 1 lists the template brains considered in this work, as well as detailing the resources available for each. Unregistered raw data, along with two template brains (one for each sex) are publicly available for FlyCircuit. The FlyLight project also provides only raw image data. Template brains and registered data are publicly available for the Vienna Tiles GAL4 libraries, but are not distributed in bulk form. We created an intersex reference brain for the FlyCircuit dataset and added spatial calibrations and re-registered data to our new template brains as necessary (see section 4.2) before constructing bridging registrations. We have deposited all template brain images, in NRRD format (`http://teem.sourceforge.net/nrrd/`) at `http://zenodo.org` to ensure long-term availability (some of the older template brains are already unavailable from their original sources). As some template brains may have multiple versions, we identify each version by its SHA-1 hash as this is uniquely dependent on the data contained in each file.

2.2 Construction of bridging registrations

Simply rescaling a sample image to match a reference brain will rarely provide usable results, due to differences in position and rotation (Figure 1a). An affine transformation can account for these differences, but does not account for differences in shape that may be of biological or experimental

origin. To correct for these, we use a full non-rigid warping deformation, as described previously (Jefferis et al., 2007; Rohlfing and Maurer, 2003; Rueckert et al., 1999). Briefly, a regular lattice of control points is created in the reference brain and corresponding control points in the sample brain are moved around to specify the deformations required to take the sample data into the reference space. Deformations between control points are interpolated using B-splines, which define a smooth deformation of sample to reference. The use of a mutual information metric based on image intensity avoids the requirement for landmarks to be added to each image a time-consuming task that can often introduce significant inaccuracies. Our approach allows for the unsupervised registration of images and the independent nature of each registration allows the process to be parallelized across CPU cores. By utilizing a high-performance computational cluster, we re-registered, with high accuracy, the entire FlyCircuit dataset within a day.

Given a bridging registration $A \mapsto B$, an attempt to produce the registration $B \mapsto A$ can be made via numerical inversion of the original registration. This is a computationally intensive process, and is not guaranteed to be successful, but we find it to be useful for neuroanatomical work as the inaccuracies are set by numerical error, which is much smaller than registration error. As the registration $A \mapsto B$ may be injective (i.e. points within brain A may map to a subset of the points within brain B), there may be some points in B, particularly near the boundaries of the brain, for which this inversion will not map them into A. To counter this we have, for some brains, constructed a new registration $B \mapsto A$ by explicitly registering B onto A, rather than relying on numerical inversion.

Full details of the constructed bridging registrations and their directions are shown in Figure 2. Here, the arrows indicate the direction of the forwards transformation but, due to the ability to numerically invert the transformations, it is possible to travel 'backwards' along an arrow to transform in the opposite direction. While the inversion takes an appreciable time to calculate, the resulting errors are extremely small, far below the resolution of the original images, and only exist due to the finite precision with which the floating-point numbers are manipulated. By inverting and concatenating bridging registrations as appropriate, it is possible to transform data registered to any of the template brains to any of the other template brains.

2.3 Construction of mirroring registrations

Whilst the *Drosophila* brain is highly symmetric it is not perfectly so and the physical handling of brains during dissection, staining and fixing can introduce further non-biological asymmetries. As such, a simple 180ř flip about the medio-lateral axis is insufficient to map a point from one brain hemisphere to the anatomically complementary point in the other hemisphere. To counter this, we have constructed non-rigid warping registrations for a number of template brains that introduce the small displacements required to fix the map from one hemisphere to the other.

After flipping, the brain will not be perfectly centered in the image and so it is first necessary to apply an affine registration to roughly match the flipped brain to the same location as the original (Figure 4a). This results in a flipped brain with the correct gross structure (i.e. large structures such as neuropils align) but with mismatched fine details (e.g. bilaterally symmetric neurons may appear to innervate slightly different regions on either side). For example, for the JFRC2 template brain we found that points are, on average, displaced by 4.8 m from their correct position, equivalent to 78 voxels of the original confocal image. The largest displacements, of the order of 1015 m, are found around the esophageal region (Figure 4b) and are likely due to specimen handling when the gut is removed during dissection.

An ideal mirroring registration would result in zero total displacement after two applications of the mirroring procedure, i.e. a point would be mapped back to exactly the same location in the original brain hemisphere. While not perfect, our constructed mirroring registrations have, on average, a round-trip displacement of less than a quarter of a micron i.e. about the diffraction limit resolution of an optical microscope and less than half of the sample spacing of the original confocal image (Figure 4c).

2.4 Mirroring examples

The *Drosophila* brain is highly laterally stereotyped, with only one asymmetric structure having been discovered so far (Jenett et al., 2012; Pascual et al., 2004). Hence, for nearly all analyses it is desirable to choose a canonical brain hemisphere and standardise such that all neurons are mapped onto this

side. This facilitates the morphological comparison of two neurons that belong to the same cell class but are located on opposite sides of the brain.

Many neurons in the *Drosophila* brain are bilateral and have arborisations in the same regions of both hemispheres. Our mirroring registrations can be used to counter non-biological asymmetries, allowing the investigation of relevant similarities and differences in morphology between the two sides of the brain. Figure 5a shows a visual projection neuron with almost perfect bilateral symmetry along with OA-VUMa2 (Busch et al., 2009) and the CSD interneuron (Dacks et al., 2006). This co-visualization facilitates the detection of differences in innervation that would be difficult to check without the mirrored counterpart, such as the higher density of innervation for the CSD interneuron in the lateral horn on the contralateral side compared to the ipsilateral lateral horn.

Our mirroring procedure does not introduce any systematic errors into neuron morphology. We have recently developed a sensitive neuron similarity algorithm, NBLAST, which we have used to calculate morphologically-determined similarity scores between DL2d projection neurons taken from the same side of the brain and compare them with those calculated between DL2d projection neurons taken from alternate sides of the brain (Figure 5b) and do not find the distributions of scores (Figure 5c) to be significantly different ($D = 0.025$, $p = 0.094$, two-sample Kolmogorov-Smirnov test). Extending this, we have used these scores to classify neurons based on their bilateral symmetry. Figure 5d shows 12 example neurons, taken from the the bilateral subset of the FlyCircuit dataset, spanning the range of similarity scores from most asymmetric (A) to most bilaterally symmetric (L). Interestingly, the distribution of scores suggest that most bilateral neurons are reasonably symmetric.

In addition to classifying neurons based on their degree of bilateral symmetry, it is also possible to use the mirroring registrations to test the degree of symmetry for sections of neurons. We take segments of a neuron and use our similarity metric to compute a score between the segment and the corresponding segment in the mirrored version of the neuron. This allows differences in innervation and axonal path between the two hemispheres to be clearly seen (Figure 5e).

2.5 Bridging examples

A successful and accurate bridging registration will result in the neuropil stains of the two template brains being well co-localized (Figure 6a). After visually inspecting the co-localized template brains to check for any obvious defects, we find it helpful to map the neuropil segmentation of Ito et al. (2014) into the space of the new brain to check for more subtle defects (Figure 6b). If the registration passes these checks it can then be used to combine data from multiple datasets.

GAL4 expression patterns of bilateral neurons with innervation in the same neuropil on either side of the brain will, in each neuropil, have contributions from both the ipsilateral and contralateral neuron. This can make it difficult to determine whether the innervation of a given neuron is denser on the ipsilateral or contralateral side. The creation of a bridge between a GAL4 expression library, such as Jenett et al. (2012), and images of single neurons, such as those of Chiang et al. (2011), facilitates the decomposition of an expression pattern into its constituent neurons, allowing the correct assessment of innervation density on the ipsilateral and contralateral sides (Figure 6c).

Similarly, correspondences between neuroblast clones can be identified with co-visualization. We bridge the Fru clones of Cachero et al. (2010) from IS2 space into the JFRC2 space of the elav clones of Ito et al. (2013) and hence determine subset relations (Figure 6d). Furthermore, we can bridge the single neuron data of Chiang et al. (2011) from the FCWB space into the IS2 space of the Fru clones and use the known sexual dimorphisms of the Fru clones to predict which neurons may be sexually dimorphic (Figure 6e, f).

The ability to bridge segmentations from one space to another is useful for checking innervation across datasets. While the single neurons of Chiang et al. (2011) were provided along with information on innervation density based on their own neuropil segmentation, this segmentation is not the same as the canonical one provided by Ito et al. (2014). We have bridged the latter segmentation into FCWB space and recalculated innervation for all the FlyCircuit neurons, providing a more standardized measure (Figure 6g).

In addition to image data, tracings of neurons can also be bridged as the registrations operate purely on 3D coordinates. We can use this, for example, to compare neurons from Chiang et al.

(2011) with those for which we have electrophysiological data (Kohl et al., 2013), enabling us to suggest a functional role for unrecorded neurons based on their morphological similarity to recorded neurons (Figure 6h).

Both the FlyLight (Jenett et al., 2012) and Vienna Tiles (http://brainbase.imp.ac.at/bbweb/) libraries contain a wealth of GAL4 lines amenable to intersectional strategies, such as that of Luan et al. (2006). However, as the two libraries are registered to different template brains, it is difficult to predict which combinations of a FlyLight line with a Vienna Tiles line would produce good results from the raw images provided by both. Bridging one library into the space of another (Figure 6i) enables direct co-visualization. This could be used manually or computationally to identify combinations that could potentially yield useful intersectional expression patterns (reviewed by Venken et al., 2011).

2.6 Interspecies deformation-based morphometry

In addition to bridging between *Drosophila melanogaster* template brains, it is possible to construct bridging registrations that take data across species boundaries. A number of gross structural sexual dimorphisms have been found in *melanogaster* brains, corresponding to regions of sexually dimorphic neuronal morphology (Kohl et al., 2013; Yu et al., 2010), especially via the use of deformation-based morphometry (Cachero et al., 2010) (see also Figure 7a–c). We hypothesized that these gross structural differences were selectively maintained during evolution. Features conserved across species would likely have broad functional significance, whilst species-specific changes may suggest an adaptive specialization. To test this hypothesis, we performed species-specific deformation-based morphometry to detect sexual dimorphisms within *Drosophila* species and bridged the detected male-enlarged regions into a common *melanogaster* template (Figure 7d–f). This clearly showed male-enlarged regions in locations consistent between all species, as well as species-specific enlargements, identifying regions of interest for further targeted study of the underlying neural circuits and their relation to behavior.

3 Discussion

We have constructed high quality registrations for the bridging of data from one template brain to another, along with registrations for mirroring data across brain hemispheres. The bridging and mirroring registrations are deposited in two version controlled repositories at http://github.com with revisions uniquely identified by the SHA-1 hash function. Since we use the distributed version control system, git, any user can clone a complete, versioned history of these repositories. We have also taken a repository snapshot at the time of the release of this paper on the publicly funded http://zenodo.org site, which associates the data with a permanent digital object identifiers (DOIs) (10.5281/zenodo.9972, 10.5281/zenodo.9973).

To simplify data access for colleagues, we have provided spatially calibrated template brains for the main template brains in use by the *Drosophila* community in a single standard format, NRRD. These brain images have permanent DOIs listed in 1. This is an open format defined at http://teem.sourceforge.net/nrrd/, again backed by open source code. NRRD images can be opened by Fiji/ImageJ, along with CMTK and a variety of image registration and medical imaging software. We have also generated registrations for the entire FlyCircuit single neuron and FlyLight datasets. The registered images have been deposited at http://virtualflybrain.org. The registrations themselves are presently available from GSXEJ they will be made available in a publication data repository on acceptance of this manuscript. Finally, we have generated new whole-brain averaged female, male and intersex*Drosophila virilis*, *yakuba* and *simulans* template brains, all of which again have DOIs.

Finally we provide two R packages, nat and nat.flybrains, that contain easy-to-use functions for manipulating 3D data in and across the main *Drosophila* template brains. Collectively, these resources enable a user to manipulate and co-visualize single neuron images and tracings, GAL4 expression patterns, neuropil segmentations and brain surfaces. The complete software toolchain for the construction and application of registrations consists exclusively of open source code released under the GNU Public License and released on http://github.com and http://sourceforge.net. A full listing of these resources is available at http://jefferislab.org/si/bridging. All of these steps will

ensure that these resources will be available for many years to come (as recommended in Ito, 2010).

Using these resources, it is now possible to combine more than 16,000 single neuron images (Chiang et al., 2011), expression patterns of > 9,500 GAL4 lines (Jenett et al., 2012; Kvon et al., 2014) and a near complete set of adult neuroblast clone lineage data (Ito et al., 2013; Yu et al., 2013). This enables direct co-visualization of single neuron, GAL4 expression and neuroblast lineages. Furthermore, our methodology and resources enable these (and future) data to be combined with the standard insect brain name nomenclature system (Ito et al., 2014). For example we have calculated the overlap between single neurons in the FlyCircuit data, which were published in 2011, and the standard neuropil domains defined in 2014. We have deposited these overlap scores with `virtualflybrain.org` who have made the data available so that they can be queried online.

We have used the same methods described to create interspecies bridging registrations within the genus *Drosophila* and have shown, via bridging into the common space of *melanogaster*, that male-enlarged regions in *melanogaster* are also present in *simulans* and *virilis*, suggesting that these sexual dimorphisms have been conserved over more than 40 million years of evolution. Species-specific male enlargements are also shown, hinting at the neurological specialization driven by the species' differing environments.

Our results suggest that template brains constructed from an average of selected high-quality brains are superior to template brains consisting of only a single brain. We therefore recommend the use of averaged brains to reduce the effects of sample-to-sample variation. Furthermore, we have found that averaged intersex template brains can form high quality registration templates for both sexes. As the number of *Drosophila* resources increases so too will the number of template brains employed, resulting in a quadratic increase in the number of potential bridging registrations. To deal with this, we propose using a small number of template brains, particularly those that are already associated with the most data, as a hub. High quality bridging registrations would be created between new template brains and brains in the hub, ensuring that any template could be bridged to any other via appropriate concatenations and inversions of these high-quality registrations. By focusing effort on ensuring that the bridges to brains in the hub are of the highest accuracy, this ensures that the cu-

mulative errors arising from the concatenation of successive registrations are minimal, giving a final registration of a higher quality than an unoptimized registration of one new template brain to another, in the same amount of time. At the present time the JFRC2 and FCWB brains are the most obvious hub brains. JFRC2 and FCWB use different counterstains, nc82 versus anti-Dlg. Although the existing bridging registration is very good it could undoubtedly be improved by generating a high quality multichannel template brain that incorporates the two counterstains.

The ability provided by these bridging registrations to combine single cell and GAL4 data will be important for developing future experiments in which control of single neurons is achieved at the genetic level. For example we have already implemented search tools that enable similarity queries of traced neurons from one dataset against another (Costa et al., 2014). We envisage that it should soon be possible to identify GAL4 lines that may contain a given neuron. The near future will see generation of electron microscopy (EM) data for the whole adult fly brain. The interpretation of high resolution EM connectomic data will be speeded and enriched by light level data. This will require EM and optical data to be bridged into a common template space using similar methodology. In this way light level single neuron "projectomes" in animals such as *Drosophila* and zebrafish may help to open up synaptic resolution connectomes. While we have concentrated on applications in *Drosophila* neuroanatomy, due to the wealth of available data, our methods will be directly applicable to other model organisms, such as zebrafish and mice, as appropriate data are released.

4 Methods

4.1 Construction of averaged template brains

CMTK's `avg_adm` tool was used to iteratively produce new averaged seed brains given a set of template brains and an initial seed brain drawn from the set. In each round, template brains are registered to the seed brain and averaged to produce a new seed brain. After all rounds are complete, a final affine registration between the latest seed brain and a flipped version is calculated and then halved, resulting in a final brain that is centered in the middle of the image. The FCWB template was produced in this

manner using 17 female and 9 male brains.

4.2 Construction of mirroring and bridging registrations

Full, non-rigid warping registrations were computed using the Computational Morphometry Toolkit (CMTK), as described previously (Jefferis et al., 2007). An initial rigid affine registration with twelve degrees of freedom (translation, rotation and scaling of each axis, Figure 1b) was followed by a non-rigid registration that allows different brain regions to move somewhat independently, subject to a smoothness penalty (Rueckert et al., 1999). In the non-rigid step, deformations between the independently moving control points are interpolated using B-splines, with image similarity being computed through the use of a normalized mutual information metric (Studholme et al., 1999). The task of finding an accurate registration is treated as an optimization problem of the mutual information metric that, due to its complex nature, has many local optima in which the algorithm can become stuck. To help avoid this, a constraint is imposed to ensure the deformation field is spatially smooth across the brain, as is biological reasonable. Full details of the parameters passed to the CMTK tools are provided in the 'settings' file that accompanies each registration.

The template brain provided by the FlyLight project (JFRC) is not spatially calibrated and so we added spatial calibration to a copy named JFRC2. Similarly, FlyCircuit images are registered to male and female template brains and so we created an intersex template brain from 17 female and 9 male brains to bring all FlyCircuit neurons into a common space, irrespective of sex. The IS2, Cell07 and T1 template brains were left unaltered.

As the neuropil and tract masks provided by the Insect Brain Name working group (Ito et al., 2014) only cover half a brain (IBN), we extended the IBN template brain into a new whole brain template (named IBNWB) to improve the quality of the bridging registration between the IBN files and the other whole brain templates. The green channel (n-syb-GFP) of the tricolour confocal data provided was taken, duplicated and flipped about the medio-lateral axis using Fiji (Schindelin et al., 2012). The Fiji plugin 'Pairwise stitching' (Preibisch et al., 2009) was used to stitch the two stacks together with an offset of 392 pixels. This offset was chosen by eye as the one from the range of offsets 385400

pixels that produced the most anatomically correct result. The overlapping region's intensity was set using the 'linear blend' method. We attempted improving on this alignment using the Fourier phase correlation method that the plugin also implements, but this gave poor results the algorithm favoured overlapping the optic lobes, with a half central brain being present on each of the left and right sides.

As the template brain is synthesized from an affine transformation of the original IBN template, we only considered an affine bridging registration between IBN and IBNWB. The n-syb-GFP labelling used in the IBN template strongly labels a large collection of cell bodies close to the cortex, posterior of the superior lateral protocerebrum and lateral horn, that are not labelled by nc82 or Dlg and hence the warping registrations from IBNWB to the other whole brain templates are less accurate in this region.

To create mirroring registrations, images were first flipped horizontally in Fiji before being registered to the original template brains using CMTK. For convenience, we also encoded the horizontal flip as a CMTK-compatible affine transformation, meaning that the entire process of mirroring a sample image can be carried in single step with CMTK.

4.3 Application of registrations to images, traced neurons and surface data

CMTK provides two commands, `reformatx` and `streamxform` that will use a registration to reformat images and transform points, respectively. The R package nat (NeuroAnatomy Toolbox) wraps these commands and can use them to transform neuroanatomical data, stored as objects in the R session, between template brains. A 3D surface model of the neuropil segmentation of Ito et al. (2014) was generated from the labelled image stack, using Amira, read into R using nat, transformed into the different template brain spaces, via JFRC2, and saved as new 3D surfaces. These can then be used to segment neurons in their original space, providing interesting volumetric data for a neuron such as the relative density of neuropil innervation.

4.4 Interspecies deformation-based morphometry

4.4.1 *Drosophila* species

We acquired 3D confocal images of the brains of four *Drosophila* species (*melanogaster*, *simulans*, *virilis*, and *yakuba*). Species were chosen on the basis of their evolutionary relationship, genomic sequence availability, and previous behavioural work . *Drosophila* stocks (obtained from N. Gompel, Institut de Biologie du Développement de Marseille-Luminy, France) were maintained at 25 řC on a standard flour-agar-yeast medium with a 12 hour light-dark cycle.

4.4.2 Immunohistochemistry

Flies were dissected in cold (1 Œ) phosphate buffer (PB) and fixed in 4 % formaldehyde fixative (400 l PB + 125 mM $NaPO_4$ [pH 7.2] + 100 l of 20 % formaldehyde [Electron Microscopy Sciences]) for 20 minutes, followed by two washes in PBT (phosphate buffered saline with 0.1 % triton). Non-specific antibody binding was blocked by incubating the brains in PBT containing 5 % normal goat serum overnight at 4 řC. nc82 staining presynaptic *brunchpilot* protein was used as a primary antibody (mouse monoclonal, 1:40) for 48 hours, followed by washing overnight, to obtain an outline of overall brain architecture. Alexa Fluor 568 (1:400) was used as a secondary antibody for 48 hours at 4 řC. After a thorough overnight wash, brains were equilibrated in Vectashield (40 l, overnight), mounted on slides and kept at 20 řC.

4.4.3 Image acquisition

3D confocal image stacks (0.46 m Œ 0.46 m Œ 1.00 m; 768 px Œ 768 px; 16-bit) were captured with a Zeiss 710 confocal microscope using an EC Plan-Neofluar 40 Œ / 1.30 NA oil objective and zoom factor 0.6. As the whole brain would not fit in one field of view, two images were stitched together, left-right, using the 'Pairwise stitching' plugin (Preibisch et al., 2009) of Fiji (Schindelin et al., 2012).

4.4.4 Reference brain generation

Intersex template brains were constructed in the same manner as described in section 4.1. 14, 10, 11 and 5 brains were used to produce averaged female template brains for *melanogaster*, *simulans*, *virilis* and *yakuba*, respectively, while 18, 11, 10 and 5 brains were used to produce averaged male template brains.

4.4.5 Deformation-based morphometry

Individual male and female brains were registered to a species-specific intersex template brain, first using a 9-degree-of-freedom affine transformation, followed by a non-rigid warping registration with a 5 m Œ 5 m Œ 5 m control point lattice (Figure 7a). After registration, the Jacobian determinant of the registration for each voxel of the reference brain was calculated and normalized (Figure 7b). We then performed an unpaired two-sample t-test on the logarithm of these values, categorized into male and female brains Cachero et al. (2010, Supplemental Information) (Figure 7c). To correct for multiple testing, thresholds were determined by using the 95th percentile of maximum t-values obtained with a permutation test ($n = 1000$) in which the sex of each brain was randomly assigned. This is preferable to methods such as Holm-Bonferroni correction which do not account for the correlation of neighbouring voxels. Due to the low number of sample brains for *yakuba*, the threshold obtained using a permutation test was greater than the highest t-value in the distribution in which the brains have the correct sex assignment and so we excluded *yakuba* from all further analysis.

4.4.6 Image analysis

Statistical image analysis was performed in R using a library of functions developed by the Jefferis group (`https://github.com/jefferis/nat.as`), wrapping CMTK commands. During image processing, Fiji (`http://fiji.sc`) was used to inspect images, Amira (`http://www.vsg3d.com/amira/`) was used for 3D visualisation.

5 Acknowledgements

We are very grateful to the original data providers including Ann-Shyn Chiang, Gerry Rubin, Arnim Jenett, Tzumin Lee, Kazunori Shinomiya and Kei Ito for generously sharing their image data with the research community. We specifically thank Arnim Jenett, Kazunori Shinomiya and Kei Ito for sharing the nc82-based *D. melanogaster* neuropil segmentation. Images from FlyCircuit were obtained from the NCHC (National Center for High-performance Computing) and NTHU (National Tsing Hua University), Hsinchu, Taiwan. We thank the Virtual Fly Brain team including MC, David Osumi-Sutherland, Robert Court, Cahir O'Kane and Douglas Armstrong for making some of our processed data available online through virtualflybrain.org. We note that data integration work with the virtualflybrain.org website was supported in part by an award from the Isaac Newton Trust to MC and Dr Cahir O'Kane

We thank members of the Jefferis lab for comments on the manuscript along with Jake Grimmett and Toby Darling for assistance with the LMB's compute cluster. This work made use of the Computational Morphometry Toolkit, supported by the National Institute of Biomedical Imaging and Bioengineering (NIBIB). This work was supported by a Starting Investigator Grant from the European Research Council, by the Medical Research Council [MRC file reference U105188491] to GSXEJ, who is an EMBO Young Investigator.

References

Avants, B., Epstein, C., Grossman, M. and Gee, J. (2008). Symmetric diffeomorphic image registration with cross-correlation: Evaluating automated labeling of elderly and neurodegenerative brain. Medical Image Analysis *12*, 26 – 41.

BRAIN Working Group (2014). BRAIN 2025: A Scientific Vision. Technical report National Institutes of Health.

Brandt, R., Rohlfing, T., Rybak, J., Krofczik, S., Maye, A., Westerhoff, M., Hege, H. C. and Menzel,

R. (2005). Three-dimensional average-shape atlas of the honeybee brain and its applications. J Comp Neurol *492*, 1–19.

Brett, M., Christoff, K., Cusack, R. and Lancaster, J. (2001). Using the Talairach atlas with the MNI template. NeuroImage *13*, 85 –.

Busch, S., Selcho, M., Ito, K. and Tanimoto, H. (2009). A map of octopaminergic neurons in the Drosophila brain. The Journal of Comparative Neurology *513*, 643–667.

Cachero, S., Ostrovsky, A. D., Yu, J. Y., Dickson, B. J. and Jefferis, G. S. X. E. (2010). Sexual dimorphism in the fly brain. Curr Biol *20*, 1589–601.

Carmack, P. S., Spence, J., Gunst, R. F., Schucany, W. R., Woodward, W. A. and Haley, R. W. (2004). Improved agreement between Talairach and {MNI} coordinate spaces in deep brain regions. NeuroImage *22*, 367 – 371.

Chiang, A.-S., Lin, C.-Y., Chuang, C.-C., Chang, H.-M., Hsieh, C.-H., Yeh, C.-W., Shih, C.-T., Wu, J.-J., Wang, G.-T., Chen, Y.-C., Wu, C.-C., Chen, G.-Y., Ching, Y.-T., Lee, P.-C., Lin, C.-Y., Lin, H.-H., Wu, C.-C., Hsu, H.-W., Huang, Y.-A., Chen, J.-Y., Chiang, H.-J., Lu, C.-F., Ni, R.-F., Yeh, C.-Y. and Hwang, J.-K. (2011). Three-dimensional reconstruction of brain-wide wiring networks in Drosophila at single-cell resolution. Curr Biol *21*, 1–11.

Christensen, G., Rabbitt, R. and Miller, M. (1996). Deformable templates using large deformation kinematics. Image Processing, IEEE Transactions on *5*, 1435–1447.

Costa, M., Ostrovsky, A. D., Manton, J. D., Prohaska, S. and Jefferis, G. S. X. E. (2014). NBLAST: Rapid, sensitive comparison of neuronal structure and construction of neuron family databases.

Dacks, A. M., Christensen, T. A. and Hildebrand, J. G. (2006). Phylogeny of a serotonin-immunoreactive neuron in the primary olfactory center of the insect brain. The Journal of Comparative Neurology *498*, 727–746.

Dreyer, D., Vitt, H., Dippel, S., Goetz, B., El Jundi, B., Kollmann, M., Huetteroth, W. and Schachtner, J. (2010). 3D Standard Brain of the Red Flour Beetle Tribolium Castaneum: A Tool to Study Metamorphic Development and Adult Plasticity. Front Syst Neurosci *4*, 3.

El Jundi, B., Huetteroth, W., Kurylas, A. E. and Schachtner, J. (2009). Anisometric brain dimorphism revisited: Implementation of a volumetric 3D standard brain in Manduca sexta. J Comp Neurol *517*, 210–25.

Grosjean, Y., Rytz, R., Farine, J.-P., Abuin, L., Cortot, J., Jefferis, G. S. X. E. and Benton, R. (2011). An olfactory receptor for food-derived odours promotes male courtship in Drosophila. Nature *478*, 236–40.

Holmes, C. J., Hoge, R., Collins, L., Woods, R., Toga, A. W. and Evans, A. C. (1998). Enhancement of MR images using registration for signal averaging. Journal of computer assisted tomography *22*, 324–333.

Ito, K. (2010). Technical and organizational considerations for the long-term maintenance and development of the digital brain atlases and web-based databases. Frontiers in Systems Neuroscience *4*.

Ito, K., Shinomiya, K., Ito, M., Armstrong, J. D., Boyan, G., Hartenstein, V., Harzsch, S., Heisenberg, M., Homberg, U., Jenett, A., Keshishian, H., Restifo, L. L., Rössler, W., Simpson, J. H., Strausfeld, N. J., Strauss, R., Vosshall, L. B. and Insect Brain Name Working Group (2014). A systematic nomenclature for the insect brain. Neuron *81*, 755–65.

Ito, M., Masuda, N., Shinomiya, K., Endo, K. and Ito, K. (2013). Systematic analysis of neural projections reveals clonal composition of the Drosophila brain. Curr Biol *23*, 644–55.

Jefferis, G. S. X. E., Potter, C. J., Chan, A. M., Marin, E. C., Rohlfing, T., Maurer, C. R. J. and Luo, L. (2007). Comprehensive maps of Drosophila higher olfactory centers: spatially segregated fruit and pheromone representation. Cell *128*, 1187–1203.

Jenett, A., Rubin, G. M., Ngo, T.-T. B., Shepherd, D., Murphy, C., Dionne, H., Pfeiffer, B. D., Cavallaro, A., Hall, D., Jeter, J., Iyer, N., Fetter, D., Hausenfluck, J. H., Peng, H., Trautman, E. T., Svirskas, R. R., Myers, E. W., Iwinski, Z. R., Aso, Y., Depasquale, G. M., Enos, A., Hulamm, P., Lam, S. C. B., Li, H.-H., Laverty, T. R., Long, F., Qu, L., Murphy, S. D., Rokicki, K., Safford, T., Shaw, K., Simpson, J. H., Sowell, A., Tae, S., Yu, Y. and Zugates, C. T. (2012). A GAL4-Driver Line Resource for Drosophila Neurobiology. Cell Rep *2*, 991–1001.

Klein, S., Staring, M., Murphy, K., Viergever, M. and Pluim, J. P. W. (2010). elastix: A Toolbox for Intensity-Based Medical Image Registration. Medical Imaging, IEEE Transactions on *29*, 196–205.

Kohl, J., Ostrovsky, A. D., Frechter, S. and Jefferis, G. S. X. E. (2013). A bidirectional circuit switch reroutes pheromone signals in male and female brains. Cell *155*, 1610–23.

Kuenzel, W. and Masson, M. (1988). A Stereotaxic Atlas of the Brain of the Chick (Gallus Domesticus). Johns Hopkins University Press.

Kurylas, A. E., Rohlfing, T., Krofczik, S., Jenett, A. and Homberg, U. (2008). Standardized atlas of the brain of the desert locust, Schistocerca gregaria. Cell Tissue Res *333*, 125–145.

Kvello, P., Løfaldli, B. B., Rybak, J., Menzel, R. and Mustaparta, H. (2009). Digital, three-dimensional average shaped atlas of the heliothis virescens brain with integrated gustatory and olfactory neurons. Frontiers in Systems Neuroscience *3*.

Kvon, E. Z., Kazmar, T., Stampfel, G., Yáñez-Cuna, J. O., Pagani, M., Schernhuber, K., Dickson, B. J. and Stark, A. (2014). Genome-scale functional characterization of Drosophila developmental enhancers in vivo. Nature *Advanced online*.

Lacadie, C. M., Fulbright, R. K., Rajeevan, N., Constable, R. T. and Papademetris, X. (2008). More accurate Talairach coordinates for neuroimaging using non-linear registration. Neuroimage *42*, 717–25.

Lefébure, M. and Cohen, L. D. (2001). Image Registration, Optical Flow and Local Rigidity. Journal of Mathematical Imaging and Vision *14*, 131–147.

Lein, E. S., Hawrylycz, M. J., Ao, N., Ayres, M., Bensinger, A., Bernard, A., Boe, A. F., Boguski, M. S., Brockway, K. S., Byrnes, E. J. et al. (2007). Genome-wide atlas of gene expression in the adult mouse brain. Nature *445*, 168–176.

Luan, H., Peabody, N. C., Vinson, C. R. and White, B. H. (2006). Refined Spatial Manipulation of Neuronal Function by Combinatorial Restriction of Transgene Expression. Neuron *52*, 425 – 436.

Pascual, A., Huang, K.-L., Neveu, J. and Préat, T. (2004). Neuroanatomy: brain asymmetry and long-term memory. Nature *427*, 605–606.

Peng, H., Chung, P., Long, F., Qu, L., Jenett, A., Seeds, A. M., Myers, E. W. and Simpson, J. H. (2011). BrainAligner: 3D registration atlases of Drosophila brains. Nat Methods *8*, 493–500.

Preibisch, S., Saalfeld, S. and Tomancak, P. (2009). Globally optimal stitching of tiled 3D microscopic image acquisitions. Bioinformatics *25*, 1463–1465.

Rein, K., Zockler, M., Mader, M. T., Grubel, C. and Heisenberg, M. (2002). The Drosophila standard brain. Curr Biol *12*, 227–31.

Rohlfing, T. and Maurer, C. R., J. (2003). Nonrigid image registration in shared-memory multiprocessor environments with application to brains, breasts, and bees. IEEE Trans Inf Technol Biomed *7*, 16–25.

Rohlfing, T., Maurer Jr, C. R., Bluemke, D. A. and Jacobs, M. A. (2003). Volume-preserving nonrigid registration of MR breast images using free-form deformation with an incompressibility constraint. Medical Imaging, IEEE Transactions on *22*, 730–741.

Rohlfing, T., Zahr, N. M., Sullivan, E. V. and Pfefferbaum, A. (2010). The SRI24 multichannel atlas of normal adult human brain structure. Human brain mapping *31*, 798–819.

Rueckert, D., Sonoda, L. I., Hayes, C., Hill, D. L., Leach, M. O. and Hawkes, D. J. (1999). Nonrigid registration using free-form deformations: application to breast MR images. IEEE Trans Med Imaging *18*, 712–21.

Schindelin, J., Arganda-Carreras, I., Frise, E., Kaynig, V., Longair, M., Pietzsch, T., Preibisch, S., Rueden, C., Saalfeld, S., Schmid, B., Tinevez, J.-Y., White, D. J., Hartenstein, V., Eliceiri, K., Tomancak, P. and Cardona, A. (2012). Fiji: an open-source platform for biological-image analysis. Nature Methods *9*, 676–682.

Studholme, C., Hill, D. L. and Hawkes, D. J. (1999). An overlap invariant entropy measure of 3D medical image alignment. Pattern recognition *32*, 71–86.

Talairach, J. and Tournoux, P. (1988). Co-planar stereotaxic atlas of the human brain. 3-Dimensional proportional system: an approach to cerebral imaging. Thieme.

Tomer, R., Denes, A. S., Tessmar-Raible, K. and Arendt, D. (2010). Profiling by Image Registration Reveals Common Origin of Annelid Mushroom Bodies and Vertebrate Pallium. Cell *142*, 800 – 809.

Venken, K. J. T., Simpson, J. H. and Bellen, H. J. (2011). Genetic manipulation of genes and cells in the nervous system of the fruit fly. Neuron *72*, 202–30.

Wullimann, M. F., Rupp, B. and Reichert, H. (1996). Neuroanatomy of Zebrafish Brain. Springer.

Yu, H.-H., Awasaki, T., Schroeder, M. D., Long, F., Yang, J. S., He, Y., Ding, P., Kao, J.-C., Wu, G. Y.-Y., Peng, H., Myers, G. and Lee, T. (2013). Clonal Development and Organization of the Adult Drosophila Central Brain. Curr Biol *23*.

Yu, J. Y., Kanai, M. I., Demir, E., Jefferis, G. S. X. E. and Dickson, B. J. (2010). Cellular organization of the neural circuit that drives Drosophila courtship behavior. Curr Biol *20*, 1602–14.

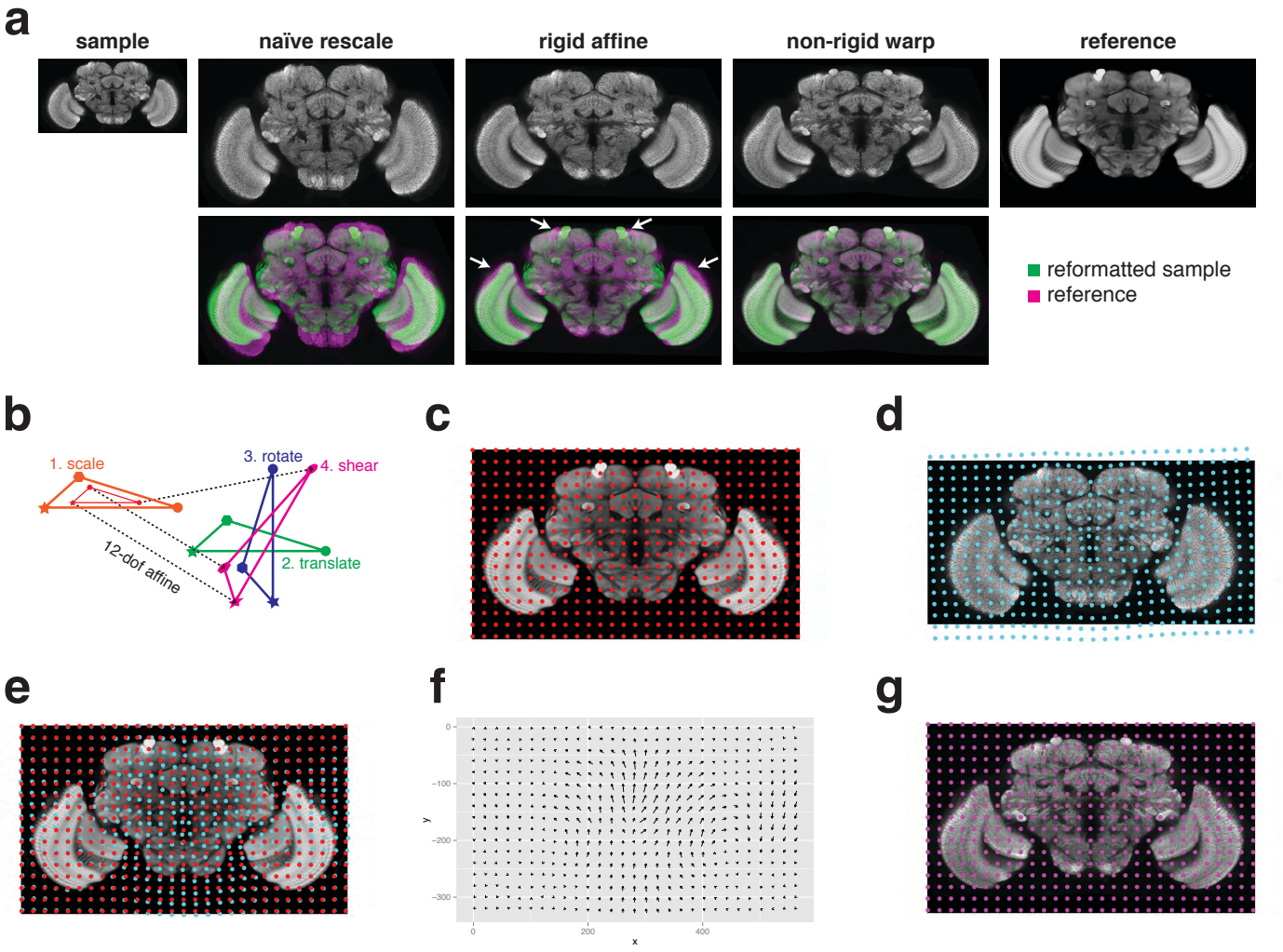

Figure 1: Registration creation procedure

a Increasing levels of registration complexity give increasingly good results. **b** Four composite transformations of a 12-degree-of-freedom affine transformation. **c** Regularly spaced grid of control points (red dots) in the reference brain. **d** Control points (cyan dots) in the sample image. **e** Sample brain control points affinely transformed into image space of reference brain, along with original control points. **f** Deformation field interpolated using B-splines. **g** Reformatted sample image.

Template Brain	Description	Citation	DOI	Resources
Wuerzburg	Single nc82-stained female brain	Rein et al. (2002)		Wild-type CantonS nc82 stained reference brain
Cell07	Partial intersex nc82-stained averaged brain (14 , 2)	Jefferis et al. (2007)	10.5281/zenodo.10570	~240 lateral horn projection neuron tracings
T1	Intersex nc82-stained averaged brain	Yu et al. (2010)	10.5281/zenodo.10590	11115 images for 6142 GAL4 driver lines from Vienna Tiles collection
IS2	Intersex nc82-stained averaged brain	Cachero et al. (2010)	10.5281/zenodo.10595	1) 1018 3d confocal images of fruitless neurons 2) 2
typical_brain_female	Single Dlg-stained female brain	Chiang et al. (2011)		~12,500 single neurons (MARCM) from FlyCircuit
typical_brain_male	Single Dlg-stained male brain	Chiang et al. (2011)		~3,500 single neurons (MARCM) from FlyCircuit
FCWB	Intersex Dlg-stained averaged brain (17 , 9)	Costa et al. (2014)	10.5281/zenodo.10568	~16,000 (see above) single neurons (MARCM) from FlyCircuit
JFRC	Single nc82-stained female brain	Jenett et al. (2012)		3,501 GAL4 driver lines from FlyLight
JFRC2	Spatially calibrated copy of JFRC	This study	10.5281/zenodo.10567	3,501 GAL4 driver lines from FlyLight,with spatial calibration
IBN	Tri-labelled half brain, with n-syb-GFP	Ito et al. (2014)		Neuropil and tract segmentations (half brain)
IBNWB	Synthetic whole-brain version of IBN	This study	10.5281/zenodo.10569	Neuropil and tract segmentations (whole brain)

Table 1: *Drosophila melanogaster* template brains
All listed template brains are available, in NRRD format, from http://jefferislab.org/si/bridging/brains/.

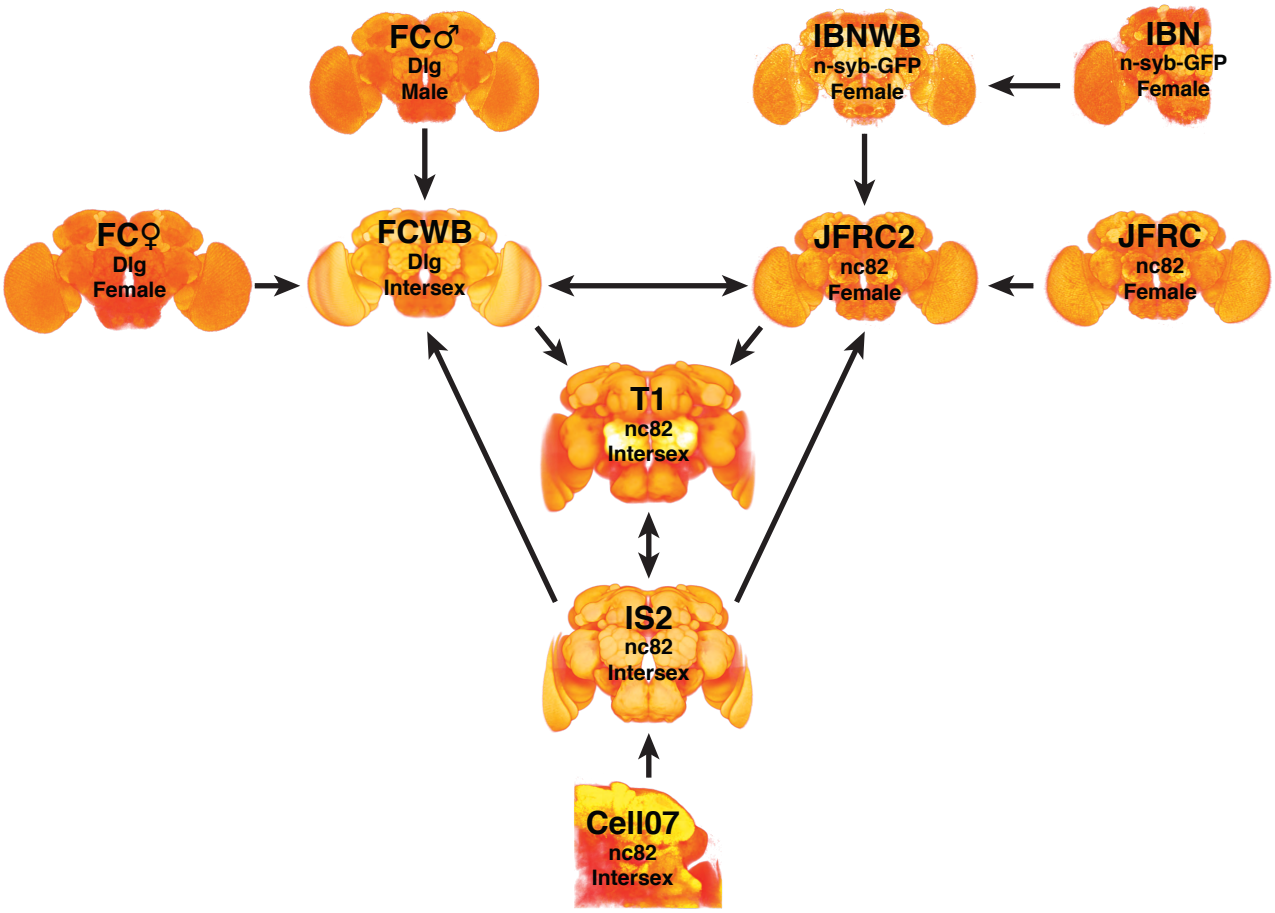

Figure 2: Bridging registrations for brain templates
Arrows indicate the existence and direction of a bridging registration. Registrations are numerically invertible and can be concatenated, meaning that the graph can be traversed in all directions. Table 1 details the template brains included.

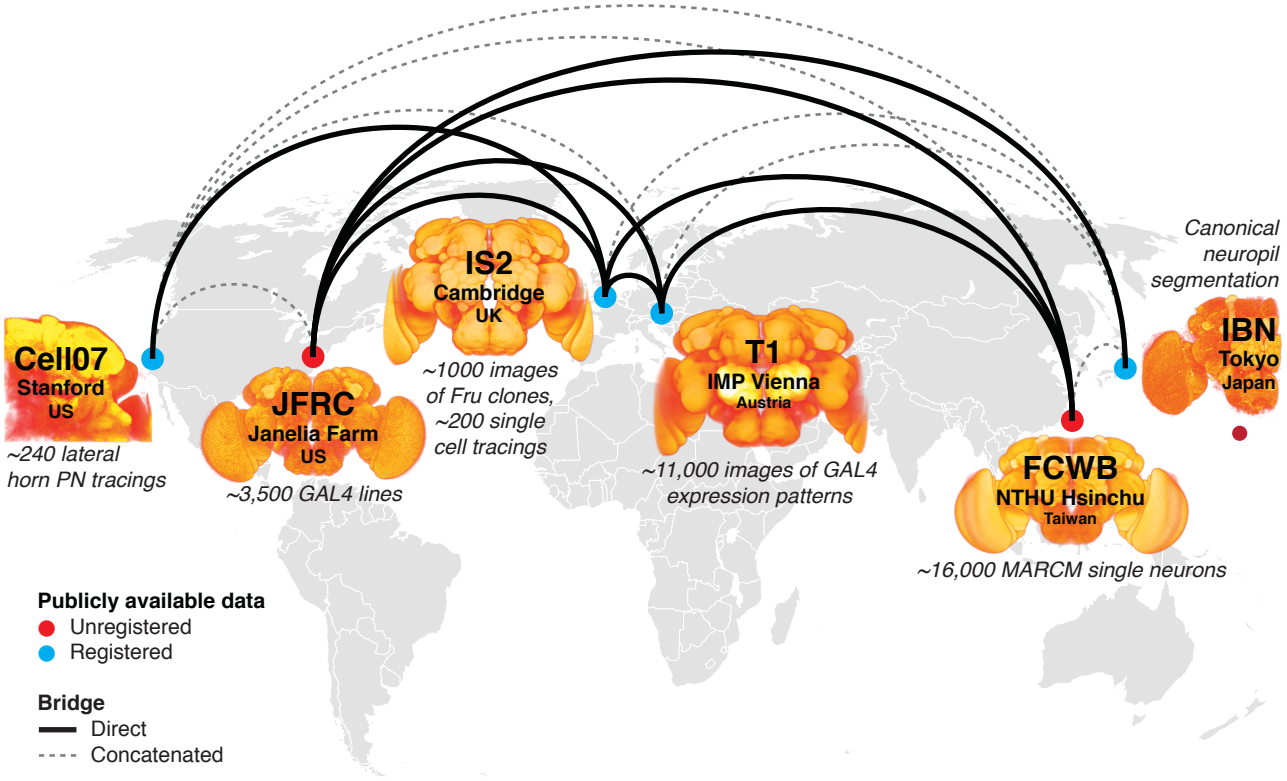

Figure 3: Bridges linking *Drosophila* neuroanatomy resources
Registered versions of publicly available unregistered data are available from virtualflybrain.org.

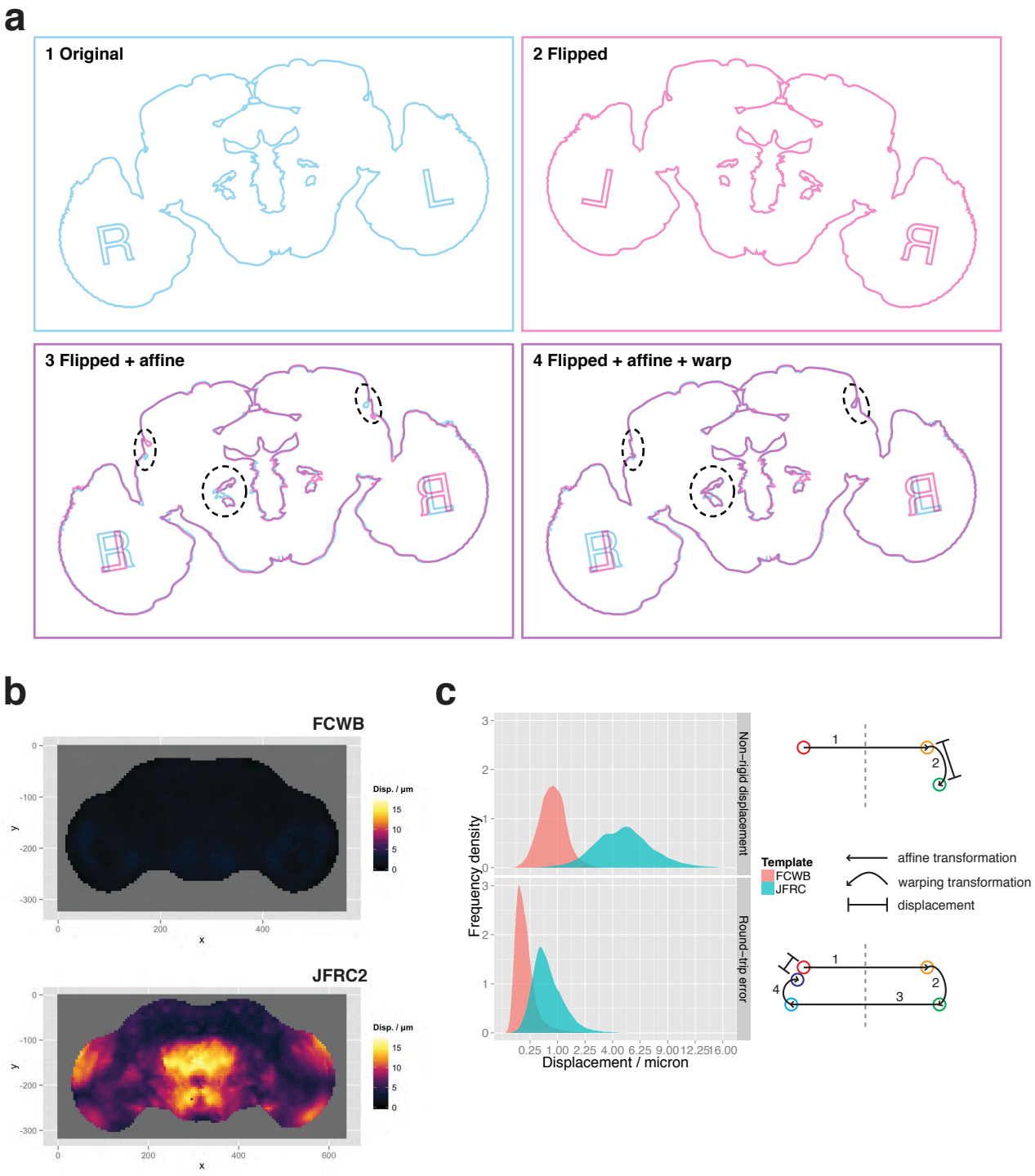

Figure 4: Mirroring procedure

a The full process undergone by an image during a mirroring registration. (1) Original image. (2) Flipped 180ř around the medio-lateral axis. (3) Affinely transformed. (4) Non-rigidly warped. **b** Heatmaps of deformation magnitude fields for mirroring FlyCircuit and FlyLight reference brains. **c** Distribution of deformation displacements for both brains, in a single mirroring operation and a full round-trip. Illustrations show the transformations that points undergo.

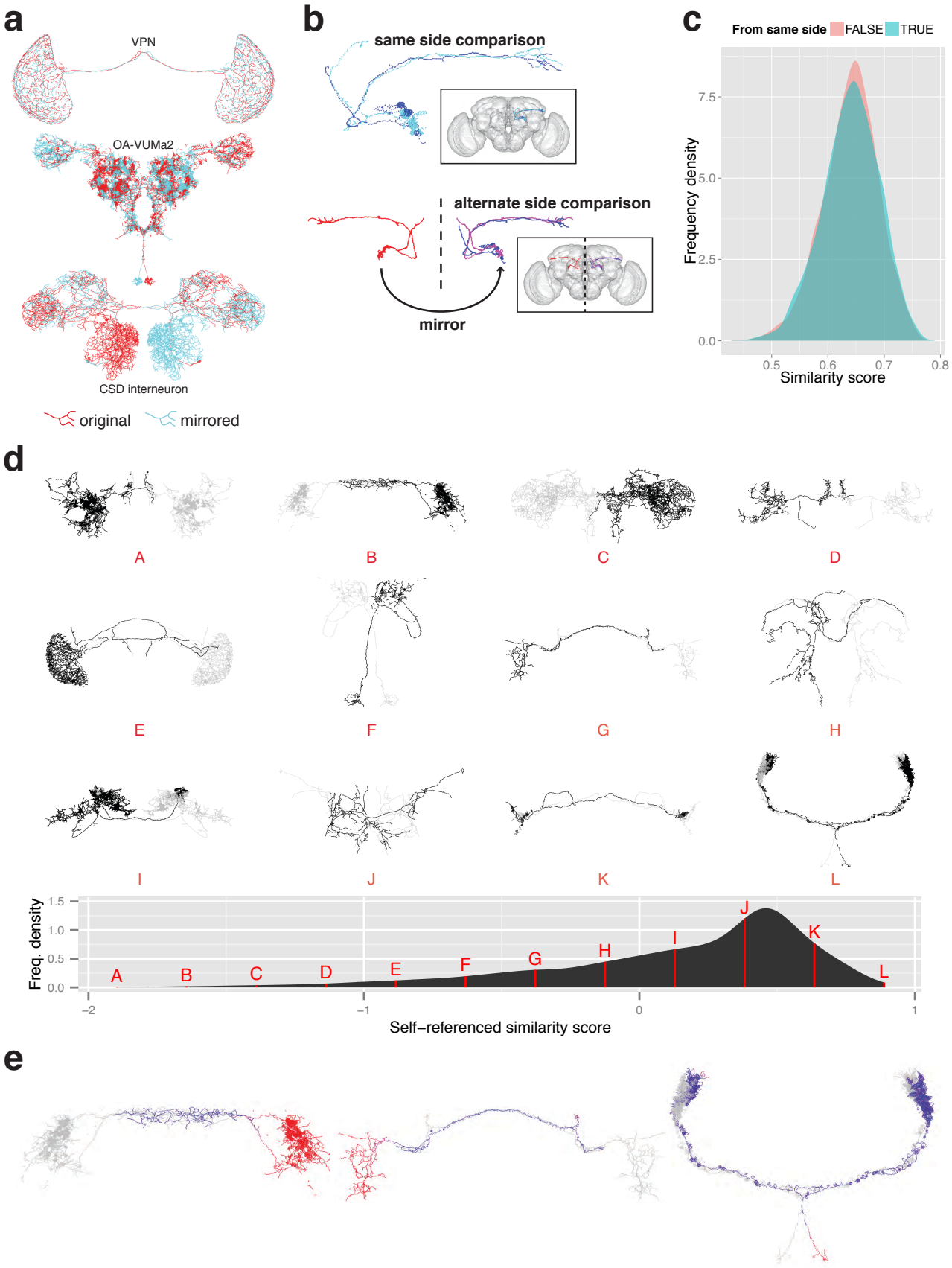

Figure 5: Sample applications of mirroring registrations

a Three FlyCircuit neurons along with mirrored versions. **b** Neurons from same side of brain and alternate side of brain are compared and a similarity score generated. **c** Distributions of similarity scores for comparisons within same brain

Figure 5: Sample applications of mirroring registrations (continued)

hemisphere and across brain hemispheres. **d** Sequence of 12 example neurons (black) with mirrored counterparts (grey), having equally spaced similarity scores. Below, full distribution of scores for all neurons in FlyCircuit dataset. **e** Segment-by-segment measures of neuron similarity. Redder shades correspond to low degrees of symmetricity, bluer shades higher. Flipped version of neuron in gray.

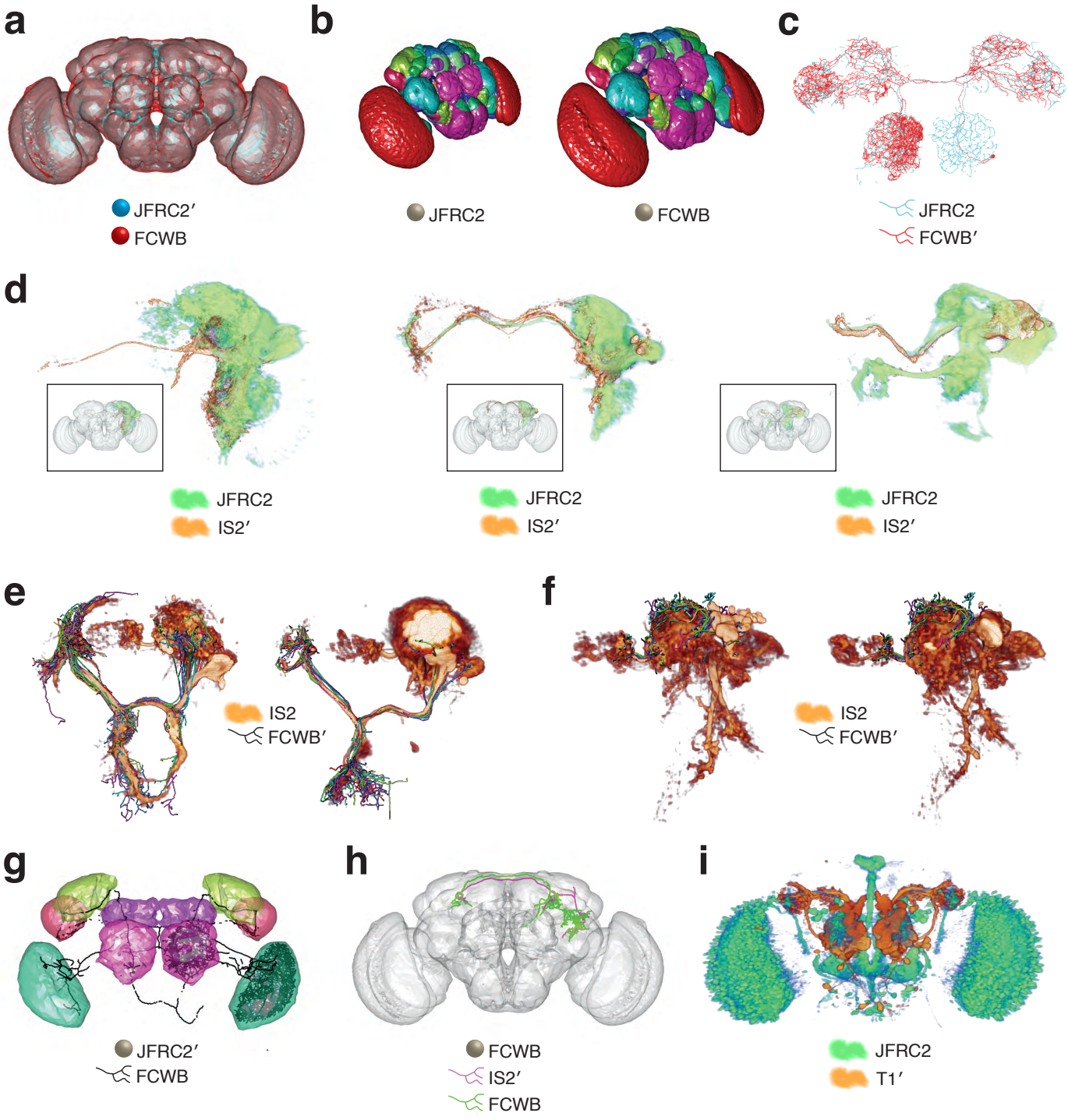

Figure 6: Sample applications of bridging registrations
Primed space names indicate original spaces for data. Unprimed space names indicate current space of image. **a** Outermost neuropil boundaries for FlyCircuit (red) and FlyLight (cyan) template brains. **b** Neuropil segmentation from JFRC2 space alongside FCWB reformatted version. **c** CSD interneuron from FlyCircuit (red) and FlyLight (cyan). **d** Fru^+ neuroblast clones (orange) transformed from IS2 space into JFRC2 space of elav neuroblast clones (green). **e** Sexually dimorphic Fru^+ neuroblast clone (male on left, female on right) along with traced neurons from FlyCircuit. **f** Non-sexually-dimorphic Fru^+ clone along with other traced neurons. **g** Neuropil segmentation from JFRC2 space in FCWB space, along with selected neurons from FlyCircuit. **h** A traced neuron in FCWB space alongside morphologically similar neuron from FlyCircuit. **i** Expression pattern of Vienna Tiles line superimposed on expression pattern of FlyLight line.

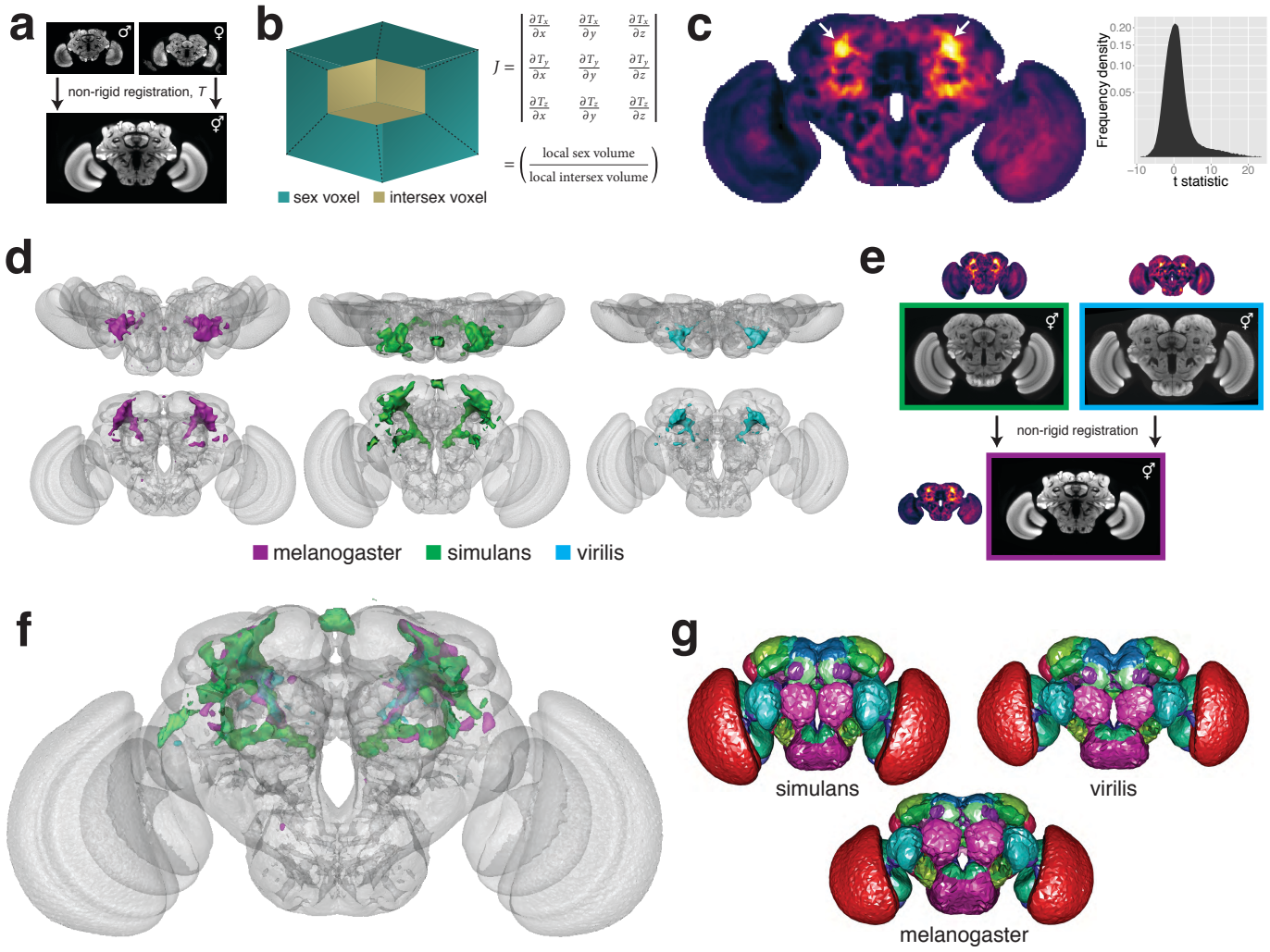

Figure 7: Interspecies deformation-based morphometry

a Male and female brains from each species non-rigidly registered to species-specific intersex template brain (*melanogaster* displayed). **b** Volume change of each voxel is noted via the use of the Jacobian determinant, *J*. **c** Jacobian determinants for female brains compared to those of male brains and used to calculate a t-statistic, in a voxel-wise manner, displayed as a heatmap. Arrows show two prominent male-enlarged regions. **d** t-values thresholded and shown as isosurfaces within each species' intersex template brain. **e** t-values non-rigidly registered into common space of *melanogaster* intersex brain. **f** Isosurfaces of d in common space of *melanogaster* template brain. **g** Neuropil segmentation of Ito et al. (2014) bridged into each species' template space.